The wavelength dependence of seeing

Robert W. Boyd*

Department of Physics, University of California, Berkeley, California 94720

(Received 30 January 1978)

The deleterious effects of atmospheric inhomogeneities on telescope angular resolution (seeing effects) were studied at a wavelength of 10 μm with an imaging upconverter. Seeing was found to be systematically better by a factor of 1.9 at 10 μm than in the visible, in good agreement with theoretical predictions. A discussion of the theory of astronomical seeing is included.

I. INTRODUCTION

The angular resolution of an astronomical telescope is often limited primarily by atmospheric turbulence, and this resolution limitation is conventionally referred to as atmospheric seeing. A systematic study of the wavelength dependence of this effect was conducted using the 1.5 m McMath solar telescope of Kitt Peak National Observatory, and this study is reported here. Telescope resolution was monitored simultaneously at wavelengths of 10 and 0.55 μm under a variety of atmospheric conditions. A high degree of correlation was found between the resolution at the two wavelengths, and the loss of resolution due to atmospheric effects was found to be systematically less by a factor of 1.9 at the longer wavelength.

The wavelength dependence of seeing effects has been a long-standing problem. Fried[1] predicted that the resolution of an astronomical telescope limited primarily by atmospheric turbulence would scale as the $\frac{1}{5}$ power of the wavelength used for observation, thus predicting better resolution in the infrared than in the visible.

A qualitative study of this wavelength dependence was conducted by Turon and Lena,[2] who used a slowly raster-scanned germanium bolometer to study solar surface features at 10 μm. They report that sunspot images are sharper at 10 μm than at visible wavelengths. Previous to the present work, however, there had been no quantitative verification of the wavelength dependence predicted by Fried.

A quantitative study of these effects was made possible by the use of a novel infrared imaging device to take pictures of the solar limb at 10 μm for subsequent comparison with visible-wavelength photographs. This imaging device, the infrared upconverter[3] shown in Fig. 1, is used to convert infrared radiation to visible radiation where it can be recorded by conventional photographic techniques. The conversion takes place by mixing the infrared signal with an intense laser beam in a nonlinear proustite crystal. The nonlinearity causes a signal to be generated whose frequency is the sum of the infrared and laser frequencies; thus the infrared signal is converted to a visible one. By a proper choice of instrumental geometry, the new sum-frequency signal will retain the spatial information present in the infrared signal, and hence infrared-to-visible image conversion takes place. A more detailed description of this instrument is found in Ref. 3.

The result that seeing degrades telescope resolution less at infrared than at visible wavelengths is of considerable importance to the field of infrared imaging, particularly for astronomical applications. With the use of the largest available telescopes it should be possible to achieve about a twofold improvement in angular resolution by using infrared rather than visible wavelengths. This suggests that recently developed infrared-imaging[3,4] and spatial-interferometry[5] techniques will prove fruitful in infrared astronomy and in other infrared detection applications. It also indicates that telescopes still larger than any presently available can be diffraction limited in the longer infrared wavelength region, and should be especially useful for infrared detection and imaging.

II. THEORY OF ATMOSPHERIC SEEING

A. Atmospheric turbulence model

Most recent theoretical work on wave propagation through a turbulent medium is based on the Kolmogorov-Obukhov model of atmospheric turbulence. Assuming the validity of this model, the wave equation is solved using either the approximation of geometrical optics, the Rytov approximation,[6] or a statistical approximation introduced by Hufnagel and Stanley.[7] Predictions of telescope resolution, image intensity fluctuations, and the wavelength dependence of each can then be derived from the model.

The atmospheric turbulence model is based on the work of Kolmogorov[8] and Obukhov[9] and is summarized in Ref. 6. These authors show that the turbulent flow can be described statistically for turbulent eddies of scale size $l \ll L$, where L is called the outer scale of the turbulent flow and is equal to the macroscopic dimensions of the flow pattern. The turbulence is damped out for eddies of size smaller than l_0, the inner scale of the turbulence. For turbulent eddies within the inertial subrange, that is for $l_0 \ll l \ll L$, the turbulence is isotropic, and its intensity depends only on the single parameter ϵ, which is the turbulent-energy dissipation rate per unit mass.

In order to describe the turbulent atmosphere in a statistical sense, it is useful to define the structure function for velocity fluctuations as

$$D_v(\mathbf{r}) = \langle [v(\mathbf{R}) - v(\mathbf{R} + \mathbf{r})]^2 \rangle, \tag{1}$$

where v is any component of the velocity vector $\mathbf{v}$, and $D_v(\mathbf{r})$ is independent of $\mathbf{R}$ for isotropic turbulence. The intensity of the turbulence depends only on the parameter ϵ, as stated above, and furthermore, the velocity difference for points separated by the distance r will be due mainly to eddies of size comparable to r. In any case, $D_v(r)$ can depend only on ϵ and r, and the only combination of these having the dimensions of $D_v(r)$ is $(\epsilon r)^{2/3}$. Thus $D_v(r) = C(\epsilon r)^{2/3}$, where C is the velocity structure coefficient. This is the "two-thirds law" of Kolmogorov and Obukhov.

More relevant to the calculation of imaging properties are

 0030-3941/78/6807-0877$00.50

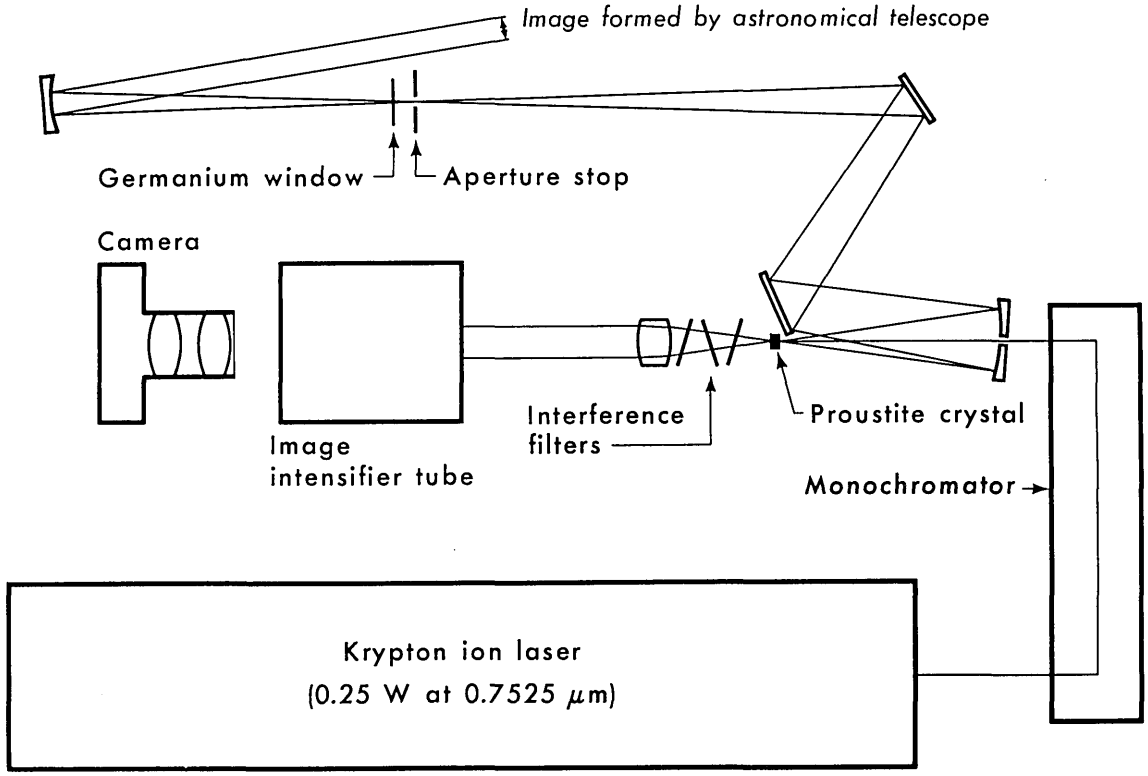

FIG. 1. Optical layout of the 10 μm imaging upconverter. The monochromator is used to eliminate background light from the laser discharge tube. Collimated infrared radiation is mixed with the laser beam in the proustite crystal. The interference filters pass the sum frequency while rejecting the laser frequency, providing a factor of 10^{18} discrimination between the two frequencies. The sum frequency image is amplified by the image intensifier tube and recorded photographically.

the statistics of the fluctuations in refractive index. These are assumed to be due to fluctuations in the air temperature, because fluctuations in pressure are assumed to come quickly to mechanical equilibrium. Temperature fluctuations are treated by assuming that local temperature is a property which is carried along by the turbulent flow, and temperature is thus known as a conservative passive additive to the flow. Temperature fluctuations δT are thus broken down by the turbulent flow to progressively smaller scales until they reach a size comparable to l_0 at which point molecular-diffusion processes even out the fluctuations. The rate at which temperature fluctuations are generated must equal the rate at which they are dissipated. This rate is given by

$$N = D\,\langle(\text{grad}\,\delta T)^2\rangle, \tag{2}$$

where D is the molecular diffusion constant.[10] The temperature structure function may be defined as

$$D_T(|\mathbf{r}|) = \langle[T(\mathbf{R}) - T(\mathbf{R}+\mathbf{r})]^2\rangle. \tag{3}$$

For $l_0 \ll r \ll L$, $D_T(r)$ can depend only on N, ϵ, and r. Dimensional analysis can again be used to show that

$$D_T(r) \sim (N/\epsilon^{1/3})r^{2/3} \tag{4}$$

or in the similar form

$$D_T(r) = C_T^2 r^{2/3}, \tag{5}$$

where C_T is the temperature structure coefficient. Similarly, one can define the refractive-index structure function as

$$D_n(|\mathbf{r}|) = \langle[n(\mathbf{R}) - n(\mathbf{R}+\mathbf{r})]^2\rangle. \tag{6}$$

Since fluctuations in n depend linearly on fluctuations in T, it follows that

$$D_n(r) = C_n^2 r^{2/3}, \tag{7}$$

where the refractive-index structure coefficient C_n is given by

$$C_n \simeq 0.1\,(P/T^2)C_T, \tag{8}$$

where T is the temperature in degrees Kelvin and P is the pressure in bars. Thus under normal conditions $C_n \sim 10^{-6}\,C_T$. While C_n is very difficult to measure, C_T can be measured in a relatively straightforward manner. Coulman[11] has measured C_T as a function of altitude using captive balloon-borne temperature sensors, and finds a wide spread in values at different times of the day, with periods of exceptionally low turbulence occasionally occurring. In order of magnitude, he measured $C_T \sim 10^{-2}$ K cm$^{-1/3}$ for the first 100 m of altitude, followed by a steady decrease toward higher altitude.

B. Calculation of imaging properties

Assuming the validity of the turbulent-atmosphere model just presented, the remaining problem is to solve the wave equation for propagation through this atmosphere. In particular, we shall need to know the modulation-transfer function (MTF) for imaging through a turbulent atmosphere whose refractive index field is described by $D_n(r) = C_n^2 r^{2/3}$, for $l_0 \ll r \ll L$. If the incident light has plane wave fronts perpendicular to the z direction, it can be described by

$$E(\mathbf{r},t) = E_0\,e^{i(kz-\omega t)}, \tag{9}$$

where E_0 is constant. After traversing the atmosphere, the wave fronts will be randomly distorted, and this wave can be

described by an equation formally identical to (9) with E_0 now a random function of t and of ρ, a vector in the plane perpendicular to the z axis. We can represent this function as

$$E_0(\rho,t) = A(\rho,t)\, e^{i\phi(\rho,t)}, \tag{10}$$

or equivalently as

$$E_0(\rho,t) = e^{l(\rho,t)+i\phi(\rho,t)}, \tag{11}$$

where l is conventionally called the log-amplitude and is given by

$$l(\rho,t) = \log_e A(\rho,t). \tag{12}$$

Fried[1] has shown that for the case of long integration times it is possible to assign an MTF to atmospheric image transmission and that the MTF for the combined optical system of the atmosphere and a telescope is given by

$$\tau(f) = \tau_0(f) \exp[(-1/2)D(\lambda Ff)]. \tag{13}$$

Here $\tau_0(f)$ is the MTF of the telescope, assumed to have focal length F, f is the spatial frequency in the focal plane, and $D(\rho)$ is the wave structure function defined as

$$(D\rho) = D_l(\rho) + D_\phi(\rho). \tag{14}$$

$D_\phi(\rho)$ is called the phase structure function and is defined as

$$D_\phi(|\rho|) = \langle[\phi(\rho') - \phi(\rho'+\rho)]^2\rangle. \tag{15}$$

The log-amplitude structure function is similarly defined as

$$D_l(|\rho|) = \langle[l(\rho') - l(\rho'+\rho)]^2\rangle. \tag{16}$$

$D(\rho)$ can be related to the statistical properties of the refractive index field by a straightforward but lengthy calculation[12] which will not be given here. This calculation yields the relation

$$D(\rho) = 2.91\, k^2 \rho^{5/3} \int C_n^2\, dz, \tag{17}$$

where $k = 2\pi/\lambda$, and the integral is taken over the propagation path. This formula is derived using the Rytov approximation[6] to the wave equation, which is strictly valid only in the limit of weak perturbations. However, the approximation seems to give good agreement with empirical evidence and includes diffraction effects. Moreover, a better approximate solution does not exist. Still, some caution should be exercised in the use of Eq. (17), especially since it is known that the weak-perturbation condition can break down. The Rytov approximation and its limits of validity are discussed further in the Appendix.

The wavelength dependence of the limiting resolution due to atmospheric distortions can readily be extracted from these equations. Throughout visible and infrared frequencies the refractive index of air changes only slightly, and thus $D(\rho)$ depends on wavelength only through k and through $\rho = \lambda Ff$. It follows that for a fixed value of the MTF, f is proportional to $\lambda^{1/5}$, indicating that better resolution should be obtained at longer wavelengths. This fact was first expressed in the literature by Fried[1] but appears never to have been experimentally verified prior to the present work. This measurement of the atmospheric MTF is described in Sec. III.

C. Empirical evidence regarding the theory of seeing

In general, the theory as outlined above has met with considerable success in experimental verification. In particular, the Kolmogorov-Obukhov model of atmospheric turbulence appears to be substantially correct, and is supported by a large amount of experimental evidence. Both $D_n(\rho)$ and $D_T(\rho)$ have been found to exhibit a $\rho^{2/3}$ dependence under general meteorological conditions.[13] Coulman[14] has measured $D_T(\rho)$ within the tunnel of the McMath solar telescope at Kitt Peak, and even under these conditions finds no substantial discrepancy from the $\frac{2}{3}$ power law.

The wave propagation predictions have met with somewhat less success, as might be expected from the fact that the Rytov approximation is expected to break down under strong turbulence. Still, the general trend has been one of experimental verification. Hufnagel and Stanley[7] found that using the best currently available average values of the temperature-structure coefficient C_T led to a seeing disk of 6 arc sec FWHM, in good factor-of-2 agreement with average daytime astronomical seeing. Coulman[15] measured the optical-transfer function over a 100 m to 1 km horizontal path while simultaneously monitoring meteorological conditions. These data were reanalyzed by Fried,[16] who used the correct theory for a spherical wave source and found exact agreement between measurement and theory, with no free parameters. Fried discussed this result in relation to the Rytov approximation, and pointed out that Coulman's data were outside the limits of applicability of geometrical optics and of first-order perturbation theory, thus suggesting that the Rytov approximation is quite good. Fitzmaurice *et al.*[17] measured the variance of the log-amplitude for horizontal propagation of 0.6328 and 10.6 μm laser beams and found the results supported the $\lambda^{-7/6}$ prediction of the Rytov approximation to Kolmogorov-Obukhov theory. An apparent breakdown of the Rytov approximation at large turbulence levels has been noted by Gracheva and Gurvich,[18] Ochs and Lawrence,[19] and Fitzmaurice[20] and has been discussed by Strobehn.[21] These authors have found that the log-amplitude variance is correctly predicted by Rytov-based theory for low variance levels, but that the variance saturates at some level, on the order of one, and no longer increases with increasing turbulence.

III. SEEING MEASUREMENTS

A. Introduction

The theory outlined in Sec. II predicts that the angular resolution of a seeing-limited astronomical telescope will improve as the $\frac{1}{5}$ power of the wavelength of observation, when the images are obtained using sufficiently long integration times. Significant improvement in image sharpness would thus be expected between the visible and the 10 μm spectral regions, since the theory predicts an improvement of 1.8. At still longer infrared wavelengths, the diffraction limit of existing telescopes could become a significant limitation to angular resolution. The scarcity of infrared imaging devices for use in astronomy undoubtedly accounts for the lack of experimental studies of angular resolution at infrared wavelengths.

Infrared and visible seeing were compared in this study by taking pictures of the Sun's limb simultaneously at 10 μm and at visible wavelengths. The sharpness of the solar limb served

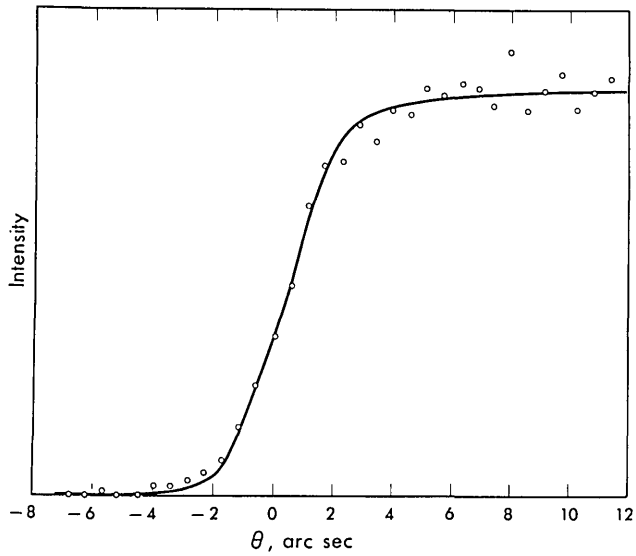

FIG. 2. Solar limb profile at 10 μm. The solid curve is a theoretical limb profile formed by convolving the true limb profile with a Gaussian-shaped point-spread function representing the combined effects of seeing, diffraction, and instrumental resolution. In this case the Gaussian has a full width to $1/e$ points of 4 arc sec.

as a measure of atmospheric seeing after corrections for differences in solar limb darkening and diffraction were made. The McMath solar telescope employs an unusually long (100 m) optical path within the telescope housing, and partly for this reason seeing is often poor for this telescope. Poor seeing, however, was desirable for this quantitative study of seeing effects. Pairs of simultaneous pictures, one at 10 μm and one at 0.55 μm wavelength, were taken under a variety of atmospheric conditions, with exposure times of 5–60 s. A good correlation between visible and infrared seeing was found, and the infrared images were found to be systematically sharper than the visible pictures. The RMS width of the point-spread function for seeing was found to be 1.9 ± 0.2 times greater at 0.55 μm than at 10 μm, in good agreement with the predictions of theory.

B. Data analysis

The raw data for this study was a series of photographic negatives showing the solar limb at 10 and at 0.55 μm. The data were put into numerical form by scanning the negatives with a PDS microdensitometer manufactured by the Boller and Chivens Division of the Perkin-Elmer Corporation. This procedure gives the transmission of the photographic negative as a function of position on the film. The film transmission is related to intensity by the characteristic curve for the photographic emulsion. A form of the characteristic curve described by de Vaucouleurs[22] was used. Position on the film can be related to angular position on the solar disk through the measured magnification of the telescope and upconverter. The result of this calibration procedure is a solar limb profile, as illustrated in the data points shown in Figs. 2 and 3.

The finite width of the transition from full to zero intensity in these limb profiles can result from several effects: seeing, diffraction, and instrumental resolution, as well as the inherently nonuniform intensity distribution of the solar disk. At visible and infrared wavelengths the Sun shows limb

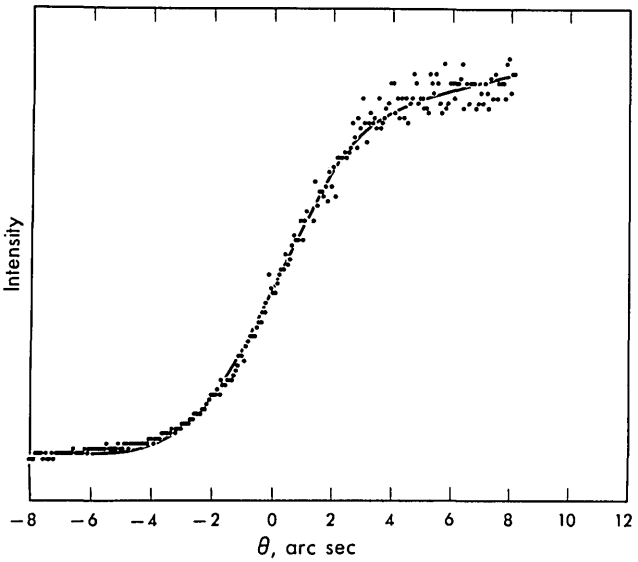

FIG. 3. Solar limb profile at visible wavelengths. The solid curve is a theoretical limb profile formed by convolving the true limb profile with a Gaussian-shaped point-spread function representing the combined effects of seeing, diffraction, and instrumental resolution. In this case, the Gaussian has a full width to $1/e$ points of 6 arc sec.

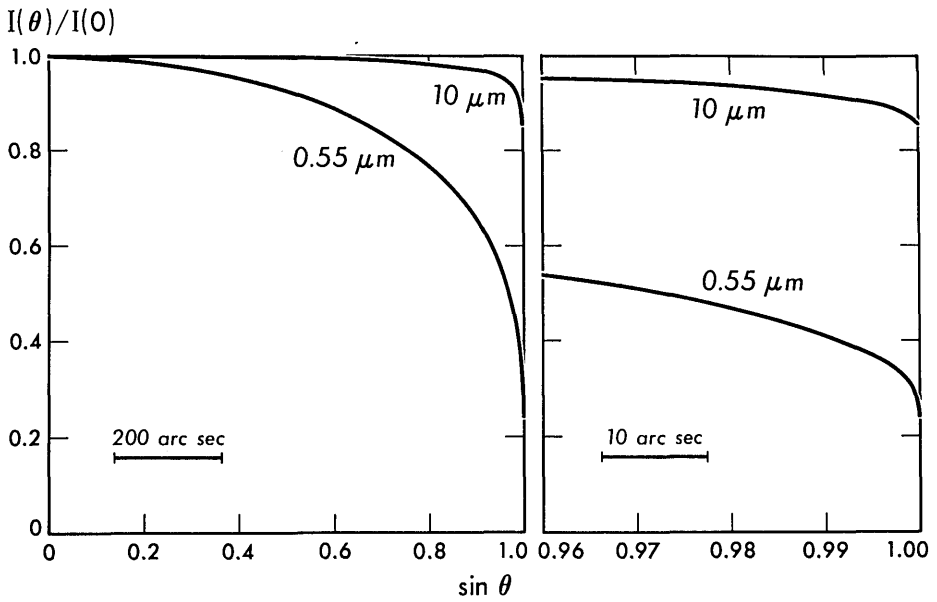

FIG. 4. Solar limb darkening at 0.55 and at 10 μm. θ is the angle at the solar surface between the Sun's radius vector and the line of sight.

darkening, as illustrated in Fig. 4. This effect has been carefully studied due to its importance in modeling the solar atmosphere.

The 0.55 μm limb darkening curve is from the work of Gaustad and Rogerson,[23] and is believed to be highly reliable. The measurements were carried out using a balloon-borne 12 in. telescope, and represent an angular resolution of 0.16 arc sec. The measurements were made at a height of 80 000 ft (24 km) in the stratosphere to minimize the effect of seeing disturbances.

The 10 μm limb-darkening curve is that of Johnson,[24] and is in fairly good agreement with that of Lena.[25] These measurements were made at the McMath telescope, and thus are affected by the problem of seeing. This is a potential source of error in the present study. However, limb darkening is a much smaller effect at 10 than at 0.55 μm, and this renders the uncertainty in the limb profile at 10 μm somewhat unimportant. In fact, to test the sensitivity of the assumed 10 μm limb profile, an alternate limb profile showing no limb darkening was employed in some of the numerical calculations, and only marginal changes in the derived seeing functions were obtained. Furthermore, Johnson did correct his limb profile as well as possible for the effect of seeing. The intensity gradient at the extreme solar limb should be nearly discontinuous at any resolution achievable from the Earth, and thus the tail of the observed limb profile can be used to estimate the point-spread function for seeing. The curve shown in Fig. 4 and used in the data analysis has the blurring effect of seeing removed by deconvolving the seeing point-spread function from the observed limb profile. This procedure becomes uncertain within 1 arc sec of the solar limb, and the data point at the limb was obtained by extrapolation.

The combined effects of diffraction and imperfect instrumental resolution were monitored by taking upconverted pictures of a resolution test pattern. To good accuracy, it was possible to assume that the instrumental (including diffraction) resolution function was a Gaussian of full width to $1/e$ points of 2.5 arc sec. Atmospheric seeing was assumed to give a Gaussian point-spread function of variable width. This width was determined by requiring that the observed limb profile be accurately represented by a model limb profile formed by convolving the true limb profile shown in Fig. 4 with the point-spread functions for instrumental resolution and for seeing. The width of the point-spread function for seeing was varied so as to minimize the sum of the squared deviations between the observed and modeled limb profiles. The quality of the fit was monitored by visual comparison between the two limb profiles. Two of these are illustrated in Figs. 2 and 3.

It is apparent from Fig. 2 that the best model profile is not a perfect fit to the observed data, especially at −3 arc sec where the model profile is too low and at +3 arc sec where the model profile is too high. This error presumably results from the assumption that the instrumental point-spread function is a Gaussian, when in fact it is the convolution of an Airy pattern with an aberration point-spread function. However, the model profile generally fits the data very well, especially in its ability to match the slope of the observed limb profile, which is the primary measure of the size of the seeing blur.

C. Results

The results of this procedure are displayed in Fig. 5. Here the width of the point-spread function for seeing at 0.55 μm is plotted against the width of the point-spread function for seeing at 10 μm. The data points represent independent measurements of the atmospheric seeing. These data were taken using integration times ranging from 16 to 60 s. Some of the data taken with shorter exposure times were sufficiently noisy that a seeing-function width could not be assigned, and these data were rejected. Also shown on Fig. 5 is a straight line of slope 1.8 which corresponds to the theoretical prediction discussed earlier. It should be noted that the data are in good qualitative agreement with this theoretical prediction, but that the data would be in poor agreement with a line of slope 1.0, corresponding to no change in seeing with wavelength.

These results can be made more quantitative by fitting a straight line to the data points with a least-squares criterion. If the line is not required to go through the origin, the best-fit straight line has a slope of 2.21 ± 0.63 and a vertical-axis in-

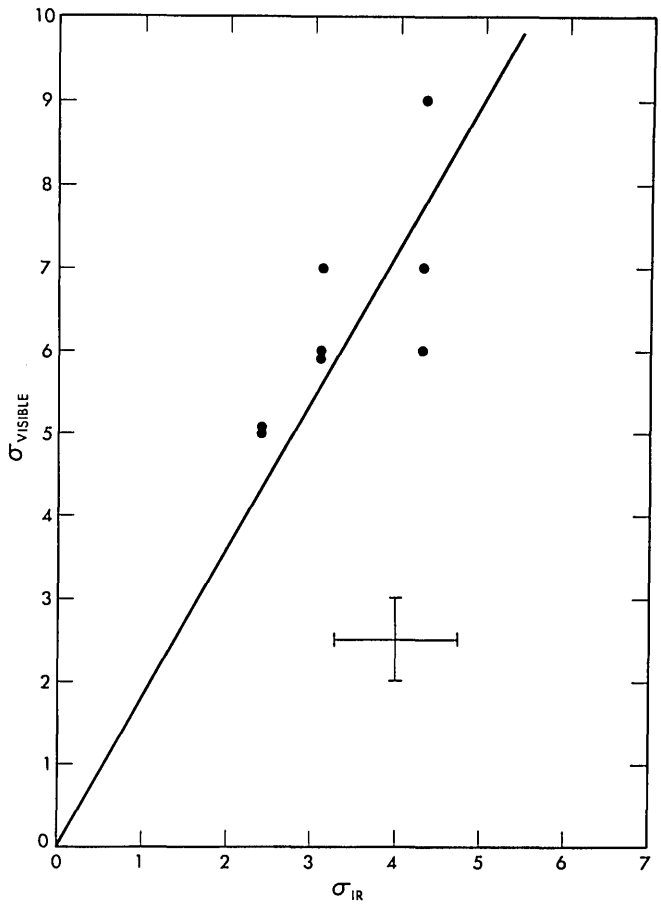

FIG. 5. Visible seeing vs infrared seeing. σ is the full width to $1/e$ points of the atmospheric MTF. The straight line of slope 1.80 corresponds to the theoretical prediction discussed in the test. A typical error bar is shown.

tercept of 0.49 ± 1.15, where standard errors are quoted. In fact the true regression must pass through the origin, because when seeing is perfect at 0.55 μm, it must also be perfect at 10 μm. With the constraint that the fitted line pass through the origin, the least-squares criterion defines a straight line more precisely, though within the rather broad limits found above. This straight line has a slope of 1.90 ± 0.20, which is in good agreement with the theoretical value of 1.80.

ACKNOWLEDGMENTS

The author acknowledges useful discussions with C. H. Townes, E. R. Wollman, and A. L. Betz. H. A. Smith and E. C. Sutton assisted with the astronomical observations. Kitt Peak National Observatory provided telescope time for this study; the support provided by the staff of this observatory is acknowledged. The PDS microdensitometer was made available by I. R. King of the Berkeley Astronomy Department. This work was partially supported by NASA Grant Nos. NGL-05-003-272 and NGR-05-003-452 and by NSF Grant No. AST 77-12256.

APPENDIX: RYTOV APPROXIMATION

This Appendix will define the Rytov approximation to the wave equation and will discuss its limits of validity, especially with regard to the prediction of seeing effects.

A plane wave $V(\mathbf{r})$ traveling in the positive z direction is assumed incident upon an inhomogeneous dielectric. The scalar wave equation for propagation through an inhomogeneous dielectric is given by

$$\nabla^2 V - \frac{n(r)^2}{c^2}\frac{\partial^2 V}{\partial t^2} = 0. \tag{A1}$$

Hufnagel and Stanley[7] show that if the fractional fluctuations in $n(r)$ are small, and if $n(r)$ does not change appreciably over distances of the order of λ, or in times of the order of λ/c, $V(\mathbf{r})$ can be expressed as

$$V(\mathbf{r}) = A_0 e^{B(\mathbf{r})} e^{i(kz-\omega t)}, \tag{A2}$$

with $B(\mathbf{r})$ satisfying the equation:

$$\nabla^2 B(\mathbf{r}) + \nabla B(\mathbf{r}) \cdot \nabla B(\mathbf{r}) + 2i\mathbf{k} \cdot \nabla B(\mathbf{r}) + 2k^2 N(\mathbf{r}) = 0, \tag{A3}$$

where

$$N(\mathbf{r},t) = [n(\mathbf{r},t) - \bar{n}(\mathbf{r})]/\bar{n}(\mathbf{r}). \tag{A4}$$

The Rytov approximation[6] entails neglecting the second term in Eq. (A3). Under this approximation, it is possible to find an analytic solution to Eq. (A3), and hence to derive an expression for the wave-structure function $D(\rho)$. Tatarski[26] gives the result

$$D(\rho) = 2.91\, k^2 \rho^{5/3} \int C_n^2\, dz, \tag{A5}$$

which is the same as Eq. (17) of this article.

Hufnagel and Stanley[7] have stated that neglecting the second term in Eq. (A3) is a somewhat dubious approximation. The second term is much smaller than the third under the assumption that $n(\mathbf{r})$ is slowly varying, and the second term is much smaller than the fourth under the assumption that $N(\mathbf{r})$ is always much less than 1. However, the second term will in general be much smaller than the first only for $|B| \ll 1$, which requires that the total phase perturbation imposed by the turbulence be small. Thus the Rytov approximation is expected to be good only for weak turbulence, and as pointed out in Sec. II E, this is qualitatively what is found.

However, the Rytov approximation is expected to be rather good under the situation of interest here. A determination of the size of the seeing disk is essentially equivalent to a determination of the maximum aperture over which the phase is coherent, or for which $|B| \leq 1$. Hence, in predicting the size of the seeing disk only the case where B is not large need be considered, and the Rytov approximation can be expected to be approximately correct, as is found empirically.

*Present address: The Institute of Optics, University of Rochester, Rochester, N.Y. 14627.

[1]D. L. Fried, "Optical resolution through a randomly inhomogenious medium for very long and very short exposures," J. Opt. Soc. Am. **56**, 1372–1379 (1966).

[2]P. J. Turon and P. J. Lena, "High Resolution Solar Images at 10 μm: Sunspot Details and Photometry," Solar Phys. **14**, 112–124 (1970).

[3]R. W. Boyd and C. H. Townes, "An Infrared Upconverter for Astronomical Imaging," Appl. Phys. Lett. **31**, 440–442 (1977), and R. W. Boyd, "Infrared Upconversion for Astronomy," Opt. Eng. **16**, 563–568 (1977).

[4]J. A. Westphal, K. Matthews, and R. J. Terrile, "Five-Micron Pictures of Jupiter," Astrophys. J. **188**, L111–L112 (1974).

[5]E. C. Sutton, J. W. V. Storey, A. L. Betz, C. H. Townes, and D. L. Spears, "Spatial Heterodyne Interferometry of VY Canis Majoris, Alpha Orionis, Alpha Scorpii, and R. Leonis at 11 Microns," Astrophys. J. **217**, L97–L100 (1977); and D. W. McCarthy, F. J. Low, and R. Howell, "Angular Diameter Measurements of α Orionis, VY Canis Majoris, and IRC +10216 at 8.3, 10.2, and 11.1 μm," Astrophys. J. **214**, L85–L89 (1977).
[6]V. I. Tatarski, *Wave Propagation in a Turbulent Medium* (McGraw Hill, New York, 1961), p. 269.
[7]R. E. Hufnagel and N. R. Stanley, "Modulation transfer function associated with image transmission through turbulent media," J. Opt. Soc. Am. **54**, 52–61 (1964).
[8]A. N. Kolmogorov, Dokl. Akad. Nauk SSSR **30**, 301 (1941); **32**, 16 (1941).
[9] A. M. Obukhov, Dokl. Akad. Nauk SSSR **32**, 19(1941); Izv. Akad. Nauk SSSR, Ser. Geograf. Geofiz. **5**, 453 (1941).
[10]V. I. Tatarski, in Ref. 6, p. 40.
[11]C. E. Coulman, "A Quantitative Treatment of Solar Seeing. I," Solar Phys. **7**, 122–143 (1969).
[12]See V. I. Tatarski, Ref. 6, Chap. 8, or J. W. Strohbehn, "Optical Propagation through the Turbulent Atmosphere," In *Progress in Optics IX*, edited by E. Wolf (North Holland, Amsterdam, 1971).
[13]J. L. Lumley and H. A. Panofsky, *The Structure of Atmospheric Turbulence* (Wiley, New York, 1964).
[14]C. E. Coulman, "A Quantitative Treatment of Solar Seeing. II," Solar Phys. **34**, 491–506 (1974).
[15]C. E. Coulman, "Optical image quality in a turbulent atmosphere," J. Opt. Soc. Am. **55**, 806–812(1965), and "Dependence of image quality on horizontal range in a turbulent atmosphere," J. Opt. Soc. Am. **56**, 1232–1238 (1966).
[16]D. L. Fried, "Test of the Rytov approximation," J. Opt. Soc. Am. **57**, 268–269 (1967).
[17]M. W. Fitzmaurice, J. L. Bufton, and P. O. Minott, "Wavelength dependence of laser-beam scintillation," J. Opt. Soc. Am. **59**, 7–10 (1969).
[18]M. E. Gracheva and A. S. Gurvich, Izv. Vyssh. Uchebn. Zaved. Radiofiz. **8**, 717 (1965).
[19]G. R. Ochs and R. S. Lawrence, "Saturation of laser-beam scintillation under conditions of strong atmospheric turbulence," J. Opt. Soc. Am. **59**, 226–227 (1969).
[20]M. W. Fitzmaurice, "Experimental Investigations of Optical Propagation in Atmospheric Turbulence," Ph.D. dissertation, University of Maryland, published as NASA TR R-370 (1971).
[21]J. W. Strobehn, in Ref. 12.
[22]G. de Vaucouleurs, "Linearization of Characteristic Curves in Photographic Photometry," Appl. Opt. **7**, 1513–1518 (1968).
[23]J. E. Gaustad and J. B. Rogerson, "The Solar Limb Intensity Profile," Astrophys. J. **134**, 323–330 (1961).
[24]N. Johnson, "Solar Infrared Limb Profiles," Ph.D. dissertation (University of Michigan, 1972) (unpublished).
[25]P. Lena, "Le Rayonnement Continu Infrarouge de la Photosphere Solaire" Astron. Astrophys. **4**, 202–219 (1970).
[26]V. I. Tatarski, in Ref. 6, Eq. (8.20).

Reconstruction of turbulence-degraded images using nonredundant aperture arrays

Timothy M. Brown
Sacramento Peak Observatory, Sunspot, New Mexico 88349*
(Received 1 October 1977)

A technique is described which allows the removal of seeing distortions from a single frame of speckle-type imagery, provided that this frame is obtained using an aperture consisting of a nonredundant array of subapertures, each smaller than the seeing correlation length. Although performed *a posteriori*, the method is related to those already proposed for use with active optical systems. Computer simulations are decribed which verify the basic features of this technique. The simulations indicate that reconstructed images of diffraction-limited quality should be obtainable for starlike objects as dim as eighth magnitude. For more extended objects, the limiting magnitude depends somewhat on the object structure. The technique described is immediately applicable to any large telescope, and because the processing is done after the fact, a frame containing many isoplanatic patches may be processed piecewise, allowing the reconstruction of large areas.

I. INTRODUCTION

Recently, several groups of workers have been pursuing the development of active optical systems aimed at removing the effects of atmospheric seeing.[1–3] One method for removing the effects of atmospheric distortion is to compute some sharpness parameter which is based on the observed intensity distribution in the image plane, and which reaches its maximum value in the absence of seeing-induced phase errors across the entrance pupil. Then, if the entrance pupil itself is divided into many independently controllable subapertures, each one smaller than the seeing correlation length, it is (in principle) a simple matter to adjust the phase at each subaperture in order to maximize the sharpness parameter, thereby cancelling the seeing distortion.

In practice, of course, this process is quite difficult. The greatest technical problems arise because seeing-induced phase perturbations change on time scales of a few milliseconds, so that the proper phase corrections for all of the subapertures must be computed and applied within this length of time. This requires apparatus of considerable complexity and sophistication. A more fundamental limitation is that the phase perturbations due to seeing are approximately constant only over regions of limited angular extent. For ground-based observations, the size of these isoplanatic patches is typically a few arc secs. Since there is only one set of phase-correcting optics, the size of the reconstructed image is limited to that of the isoplanatic patch, which in many applications is a serious impediment. One can imagine ways around this problem, but only at the expense of multiple optical systems or low duty cycles, neither of which is desirable.

These difficulties suggest that it would be useful to perform the phase correction *a posteriori*, on an already recorded

 0030-3941/78/6807-0883$00.50